

COMPARISON OF METHODS FOR MODELING UNCERTAINTIES IN A 2D HYPERTHERMIA PROBLEM

D. Voyer, L. Nicolas, and R. Perrussel

Laboratoire Ampère (UMR CNRS 5005)
Université de Lyon
École Centrale de Lyon, 36 avenue Guy de Collongue
Ecully 69134, France

F. Musy

Institut Camille Jordan (UMR CNRS 5208)
Université de Lyon
École Centrale de Lyon, 36 avenue Guy de Collongue,
Ecully 69134, France

Abstract—Uncertainties in biological tissue properties are weighed in the case of a hyperthermia problem. Statistical methods, experimental design, kriging technique, stochastic methods, and spectral and collocation approaches are applied to analyze the impact of these uncertainties on the distribution of the electromagnetic power absorbed inside the body of a patient. The sensitivity and uncertainty analyses made with the different methods show that experimental designs are not suitable for this kind of problem and that the spectral stochastic method is the most efficient method only when using an adaptive algorithm.

1. INTRODUCTION

An important issue in hyperthermia and more generally in numerical dosimetry tackles the variability of the biological tissue properties [1]. This variability can be modeled by considering those properties as *random variables* with probabilistic laws in agreement with the existing experimental data. The problem consists then in evaluating how this uncertainty affects physical quantities such as the distribution of the electromagnetic power absorbed inside the human body. In this work,

some variability is introduced for the biological tissue properties in a hyperthermia problem. Even if 3D situations are more realistic, a 2D example has been chosen here for focusing the study mainly on the variability aspect. In order to determine the *most influential factors* and *quantify their effects*, different approaches are briefly presented and compared in terms of accuracy and computational cost: a two level experimental design approach [2], kriging approach [3] and finally, stochastic spectral [4] and collocation [5] methods using adaptive sparse grid [6].

2. HYPERTHERMIA PROBLEM

The treatment of a tumor located inside the liver of a patient is considered. The 2D model has been obtained from a computed tomography slice of the body.

In the *first step*, the electromagnetic properties (permittivity ϵ and conductivity σ) of the different healthy tissues are set to the common values used in literature [7] while those of the tumor are based on a specific study of cancerous tissues at radio frequencies [8] (see Table 1). The amplitudes and the phases of four incident waves are adjusted so that to maximize the power absorbed inside the liver and minimize the power absorbed elsewhere in the body (see Fig. 1). More precisely, the quantity we minimize is:

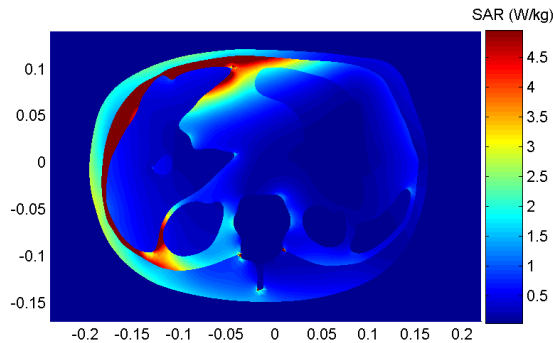


Figure 1. Repartition of the specific absorption rate (SAR) inside the body when it is illuminated by four incoming waves. The frequency is set to 100 MHz. Computations are performed using the finite element library getfem++ [9].

Table 1. Mean values of tissue parameters involved in the hyperthermia problem and range of variation.

Quantity	Mean	Variation
σ muscle	0.707	$\pm 25\%$
ϵ_r muscle	65.972	$\pm 25\%$
σ fluid body	1.504	$\pm 25\%$
ϵ_r fluid body	69.085	$\pm 25\%$
σ bone	0.064	$\pm 25\%$
ϵ_r bone	15.283	$\pm 25\%$
σ marrow	0.022	$\pm 25\%$
ϵ_r marrow	6.488	$\pm 25\%$
σ kidney	0.810	$\pm 25\%$
ϵ_r kidney	98.094	$\pm 25\%$
σ liver	0.487	$\pm 25\%$
ϵ_r liver	69.022	$\pm 25\%$
σ tumor	1.005	$\pm 50\%$
ϵ_r tumor	84.342	$\pm 50\%$
σ bowel	1.655	$\pm 25\%$
ϵ_r bowel	96.549	$\pm 25\%$
σ lung	0.558	$\pm 25\%$
ϵ_r lung	67.108	$\pm 25\%$

$$y = \frac{\int_{\text{body} \neq \text{liver}} \sigma(\tau) |E(\tau)|^2 d\tau}{\int_{\text{liver}} \sigma(\tau) |E(\tau)|^2 d\tau} \quad (1)$$

where E is the amplitude of the electric field. As it is not the core of this work, this optimization step will not be detailed.

In the *second step*, the properties of the different tissues are supposed to be random variables with uniform probability laws while the phases and amplitudes of the four incident waves are maintained at the values found in the first step. For the sake of illustration, the properties of the tissues are assumed to vary in a range of $\pm 25\%$ around the mean value except those of the tumor, which vary in a range of $\pm 50\%$; this distinction is introduced because the properties of tumors are usually less known than those of healthy tissues.

In the following, y , defined in (1) as the observed quantity, is a random variable depending on the 18 random variables corresponding

to the tissue properties. For each of the strategies mentioned in the introduction, a *specific model* for y is assumed and a *specific numerical experimental design* is built in order to estimate the unknown parameters of the model. Such a design consists in the choice of a set of realizations or *nodes* for the random variables. Comparisons are proposed in terms of sensitivity and uncertainty analyses.

3. CLASSIC TWO LEVEL EXPERIMENTAL DESIGN

The random input variables are normalized between -1 , the low level, and $+1$, the high level. The model for y is:

$$y(\tilde{\mathbf{x}}) = \beta_0 + \sum_{i=1}^{18} \beta_i \tilde{x}_i + \sum_{i=1}^{18} \sum_{j>i} \beta_{i,j} \tilde{x}_i \tilde{x}_j + \dots + \epsilon(\tilde{\mathbf{x}}) \quad (2)$$

where $\tilde{\mathbf{x}} = \{\tilde{x}_i\}_{i=1,\dots,18} \in [-1, 1]^{18}$ denote the normalized variables. The coefficients $\{\beta_i\}_{i=1,\dots,18}$ correspond to the main components; $\{\beta_{i,j}\}_{i,j=1,\dots,18; j>i}$ correspond to the interactions between two variables; higher order interactions are also considered. The first part of the model is the *regression model* and the remaining ϵ is the *error*. This error is supposed to be a random process with a *zero mean* and where *two realizations are uncorrelated*.

Once a numeric experimental design is built, the estimate $\hat{\beta}$ of β is the *ordinary least square solution* based on the nodes of the design. In statistics, it is also the *best linear unbiased predictor* for β .

In a *two level experimental design*, the nodes are chosen at the edges of the domain and thus each \tilde{x}_i can take the values -1 and $+1$. Consequently, the complete design will involve $2^{18} = 262,144$ nodes. When the numerical experiments are expensive in computational resources, the complete design cannot be performed. A solution is to consider fractional experimental designs where some effects are confounded. A fractional design is characterized by its resolution: in a resolution III, main components can be confounded with interactions of order 2; in a resolution IV, main components cannot be confounded with interactions of order 2 but two interactions of order 2 can be confounded.

Fractional designs of resolution III and IV have been applied to the hyperthermia problem. The results are detailed in Table 2. Our attention is focused on the most influential components even though an experimental design enables to also extract information on the interactions between factors. As the quality of the resolution increases, the cost also increases: 32 nodes for a resolution III and 64 nodes for a

resolution IV. It appears that *the properties of the liver and the fluid body have the greatest influence* on the value of y ; the properties of the muscle have a lower impact. As shown in the next sections, these results are in agreement with those obtained by other methods. On the other hand, the experimental designs give little importance to the properties of the tumor and the bone, which is actually unexpected. Moreover, there is a discrepancy in the estimation of the coefficients β_6 and β_{14} between resolution III and IV. In order to refine the results, the resolution should be increased but the numerical cost will also strongly increase: 512 nodes is required for the resolution VI (resolution V does not exist for this example).

Table 2. Results for the fractional experimental design.

Quantity	Coefficient	Resolution III 2^{18-13} 32 nodes	Resolution IV 2^{18-12} 64 nodes
	β_0	16.888	17.194
σ muscle	β_1	3.378	2.514
ϵ_r muscle	β_2	-1.222	-2.0237
σ fluid body	β_3	5.976	6.812
ϵ_r fluid body	β_4	-5.348	-5.485
σ bone	β_5	1.035	0.845
ϵ_r bone	β_6	-0.796	0.508
σ marrow	β_7	0.331	-0.538
ϵ_r marrow	β_8	-0.485	0.297
σ kidney	β_9	0.150	-0.309
ϵ_r kidney	β_{10}	0.124	0.231
σ liver	β_{11}	-5.421	-5.935
ϵ_r liver	β_{12}	4.679	4.930
σ tumor	β_{13}	-1.812	-1.689
ϵ_r tumor	β_{14}	-1.565	1.322
σ bowel	β_{15}	-0.408	-0.249
ϵ_r bowel	β_{16}	0.179	-0.409
σ lung	β_{17}	-0.215	-0.120
ϵ_r lung	β_{18}	0.530	0.119

Table 3. Results for the kriging approach: partial variance (%) and total effect (%) of the different parameters.

Quantity	40 nodes		100 nodes	
	Variance	Effect	Variance	Effect
σ muscle	2.40	2.79	2.14	2.35
ϵ_r muscle	2.82	3.59	1.25	1.51
σ fluid body	29.26	34.25	27.06	31.86
ϵ_r fluid body	17.56	21.72	19.90	24.74
σ bone	0.20	0.28	0.01	0.05
ϵ_r bone	0.14	0.14	0.02	0.05
σ marrow	0.44	0.51	0.04	0.04
ϵ_r marrow	0.05	0.25	0.03	0.07
σ kidney	0.24	0.24	0.01	0.01
ϵ_r kidney	0.14	0.25	0.03	0.04
σ liver	20.02	22.17	22.85	25.91
ϵ_r liver	18.00	19.15	17.77	19.87
σ tumor	0.59	0.75	0.16	0.41
ϵ_r tumor	0.29	0.29	0.25	0.87
σ bowel	0.49	0.62	0.04	0.49
ϵ_r bowel	0.13	0.13	0.03	0.24
σ lung	0.11	0.14	0.04	0.35
ϵ_r lung	0.09	0.09	0.04	0.17

4. KRIGING

In the kriging approach, the model of y is composed of a regression model, as in classic experimental design, and of an error whose properties are different from the error given in (2). Indeed, the error is chosen to be a stationary Gaussian process with a *zero mean* but where *two realizations are correlated*. From the numeric experimental design, the parameters of the correlation function are estimated and it enables to correct the systematic bias that appears between y and the regression model at the nodes of the design.

The software *GEM-SA* [10] is used to test the kriging method. To compute the model of y , it generates a *Latin hypercube design* of the initial hypercube with 18 dimensions. For a user-defined number of

nodes, this Latin hypercube is the result of an optimization process of the *space-filling properties*.

Two simulations of the hyperthermia problem have been carried out using 40 nodes and 100 nodes. The sensitivity analysis is given in Table 3. For each input random variable x_i , the partial variance and the total effect are computed; those quantities correspond respectively to $\text{Var}[E[y|x_i]]/\text{Var}[y]$, where $E[\cdot]$ denotes the expectancy and $\text{Var}[\cdot]$ the variance, and to the contribution to the variance of x_i but also of the higher order interactions involving x_i [11]. It appears that *the properties of the fluid body and the liver are the most influential parameters* on y . The muscle also has an effect but less important. The other variables do not have any influence on y . In particular, the contribution of the tumor is insignificant: this is due to the fact that the tumor is small and consequently, its influence on the integral in (1) is negligible. Moreover, it seems that there is *low coupling* between the different variables since *the partial variance is close to the total effect*. As for the mean and the variance, the results are in accordance with those obtained in the next sections (see Table 4).

5. STOCHASTIC SPECTRAL METHOD

The stochastic spectral method is based on the expansion of the random variable y in a polynomial basis depending on the input random variables. Since the input random variables are characterized by uniform laws, it can be efficiently expanded on the generalized polynomial chaos [12] based on the Legendre polynomials:

$$y(\boldsymbol{\xi}) = \sum_{\mathbf{i} \in \mathbb{N}^{18}} y_{\mathbf{i}} \Psi_{\mathbf{i}}(\boldsymbol{\xi}) \quad \text{with} \quad \Psi_{\mathbf{i}}(\boldsymbol{\xi}) = \prod_{k=1}^{18} L_{g_{i_k}}(\xi_k). \quad (3)$$

The L_{gp} are the Legendre polynomials and $\boldsymbol{\xi} = \{\xi_k\}_{k=1, \dots, 18}$ the normalized input random variables with uniform laws defined on $[-1, 1]$. The *total degree* of the polynomial is the sum of the indexes i_k in (3).

The unknown coefficients $y_{\mathbf{i}}$ in (3) can be computed using the projection method:

$$y_{\mathbf{i}} = \frac{E[y \Psi_{\mathbf{i}}]}{E[\Psi_{\mathbf{i}}^2]} = \frac{1}{E[\Psi_{\mathbf{i}}^2]} \int_{[-1, 1]^{18}} y(\boldsymbol{\xi}) \Psi_{\mathbf{i}}(\boldsymbol{\xi}) \frac{1}{2^{18}} d\boldsymbol{\xi}. \quad (4)$$

The term $E[\Psi_{\mathbf{i}}^2]$ can be computed analytically but to compute the second integral in (4), quadrature rules are applied; this will define the

numerical experimental design. This *scientific computing approach* is quite different from the *statistical approach* using Latin hypercubes discussed in the previous section. However, applying a tensor product design based on one-dimensional Gaussian quadrature rules is most of the time prohibitive since the number of quadrature nodes increases exponentially with the number of dimensions. For instance, an exact integration up to the order 7 requires $4^{18} = 68,719,476,736$ simulations. This number can be dramatically reduced using a *sparse grid*: only 9,841 have to be computed when considering Smolyak's algorithm with *Gauss Patterson nodes*. Nonetheless, an *adaptive sparse grid algorithm* is even more suited in order to explore only the most influential factors. This technique is used with Gauss Patterson nodes since their building relies on *nested sequences* at the different levels of accuracy [6]. However, another choice of quadrature nodes is possible with some limitations: Stroud nodes can give the same results with less computations when the degree of polynomials in (4) is low [5, 13].

Our criterion for adaptivity in the hyperthermia problem is *based on the variance*. From (3), the variance is given by:

$$\sigma_y^2 = \sum_{\mathbf{i} \in \mathbb{N}^{18} \setminus (0, \dots, 0)} y_{\mathbf{i}}^2. \quad (5)$$

In the adaptive version of Smolyak's algorithm (see Appendix A for more details), a comparison of the increment of variance brought by each direction provides the error indicator allowing to choose in which direction the accuracy of the quadrature has to be increased. A direction in the algorithm is described by the index $\mathbf{i} = [i_1, \dots, i_{18}]$ where the k -th component is such that $i_k + 1$ indicates a level of accuracy of the quadrature rule following the k -th variable. In (5), the sum is reduced to the indexes \mathbf{i} for which the numerical integration of $E[\Psi_{\mathbf{i}}^2]$ is exact. At the beginning of the algorithm, only one point is computed and it corresponds to the index $[0, \dots, 0]$. At this stage, only the term y_0 can be estimated and no term is available to calculate the variance in (5). At the first iteration of Smolyak's algorithm, the level of accuracy is increased successively for each variable i.e., from index $[1, 0, 0, \dots, 0]$ to $[0, 0, \dots, 0, 1]$. At this step, only the coefficients related to the polynomials of total degree less or equal to 1 are calculated from (4). Then, the variance in (5) is reduced to a sum of 18 terms. At the second iteration of Smolyak's algorithm, the level of accuracy is increased from the direction that has brought the largest contribution to the variance. The new sequences are used not only to refine the calculation of existing $y_{\mathbf{i}}$ coefficients but also to integrate new $y_{\mathbf{i}}$ coefficients that can be computed more precisely with

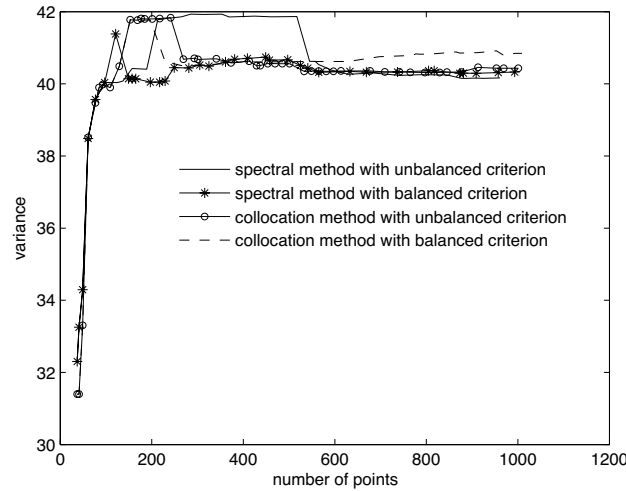


Figure 2. Convergence of the stochastic spectral and collocation methods using balanced and unbalanced criterions.

the new nodes. This approach can be seen as an *adaptive building of the polynomial chaos*.

Figure 2 shows the convergence study of the stochastic spectral method. Two criteria have been experimented in the adaptive algorithm: first, only the contribution of an index to the variance is considered; second, the contribution of an index to the variance is balanced by the number of new nodes to calculate, i.e., the computing time cost of the new nodes is taken into account. It appears that the convergence is better when using the balanced variance criterion: in this case, the variance converges after about 150 nodes while it needs more than 400 nodes in the case of the unbalanced criterion. The variance converges to a value close to the result obtained with the kriging technique (see Table 4). However, the stochastic method gives

Table 4. Mean and variance computed using the different methods.

Method	Kriging		Stochastic spectral		Stochastic collocation		
	Nb. of nodes	40	100	150	1,000	160	1,000
Mean	41.558	42.518	40.140	40.341	39.786	40.846	40.138
Variance	14.082	14.218	14.138	14.131	14.131	14.135	14.135

Table 5. Results for the stochastic spectral method: partial variance (%) and total effect (%) of the different parameters.

Quantity	150 nodes		1000 nodes	
	Variance	Effect	Variance	Effect
σ muscle	2.80	3.20	2.79	3.29
ϵ_r muscle	1.82	2.16	1.80	2.16
σ fluid body	28.19	32.34	27.86	32.50
ϵ_r fluid body	19.88	23.50	19.58	23.54
σ bone	0.00	0.00	0.00	0.00
ϵ_r bone	0.00	0.00	0.00	0.00
σ marrow	0.00	0.00	0.00	0.00
ϵ_r marrow	0.00	0.00	0.00	0.00
σ kidney	0.00	0.00	0.00	0.00
ϵ_r kidney	0.00	0.00	0.00	0.00
σ liver	23.89	26.60	23.67	26.78
ϵ_r liver	16.12	17.91	15.89	18.00
σ tumor	0.10	0.10	0.28	0.50
ϵ_r tumor	0.52	0.67	0.50	0.89
σ bowel	0.02	0.02	0.03	0.03
ϵ_r bowel	0.03	0.03	0.04	0.04
σ lung	0.00	0.00	0.00	0.00
ϵ_r lung	0.00	0.00	0.00	0.00

a more accurate result with about one hundred nodes than the kriging method. The sensitivity analysis is reported in Table 5: the data are in agreement with those obtained by the kriging method. Three tissues impact on the variability of y : the fluid body, the liver and the muscle. The others are nearly negligible and their influence is more residual than in the kriging prediction.

6. STOCHASTIC COLLOCATION METHOD

Sparse grid with an adaptive algorithm can also be exploited to interpolate y . In this case, the interpolation function is obtained using multi-dimensional Lagrange polynomials and it can be efficiently built not only from Gauss Patterson nodes but also from other nodes like

Stroud or Chebyshev nodes. As the sequences of nodes are nested, the error indicator on the value of y at new nodes can be given by the absolute difference with the values interpolated using the older nodes.

In this section, we use the Matlab *sparse grid interpolation toolbox* [14]. As in the previous section, the adaptivity criterion can be or not be balanced by the numerical cost of a sequence. Both situations have been carried out and the results are given in Fig. 2. It appears that the results do not converge exactly to the same value: with 1,000 nodes, $\sigma_y^2 = 40.434$ for the unbalanced criterion whereas $\sigma_y^2 = 40.846$ for the balanced one. The result with the unbalanced criterion is closer to the result given by the stochastic spectral method. Moreover, it seems that the convergence is achieved later compared to the stochastic spectral method. This is probably due to the fact that the collocation method adaptivity used here is related to the quality of the interpolation whereas the spectral method adaptivity is directly linked to the variance. The effect of the different strategies can also be viewed when one is interested in the maximum polynomial order reached in the 18 variables. Fig. 3 shows this result after 1,000 nodes for the spectral and collocation methods. In both cases, the most influential variables (number 1, 2, 3, 4, 11 and 12) are largely explored. The variables associated to the tumor properties (number 13 and 14) are also exploited because of their weaker but existing influence. However, the collocation method goes further in the exploration of the variable number 16 that corresponds to the bowel permittivity but this

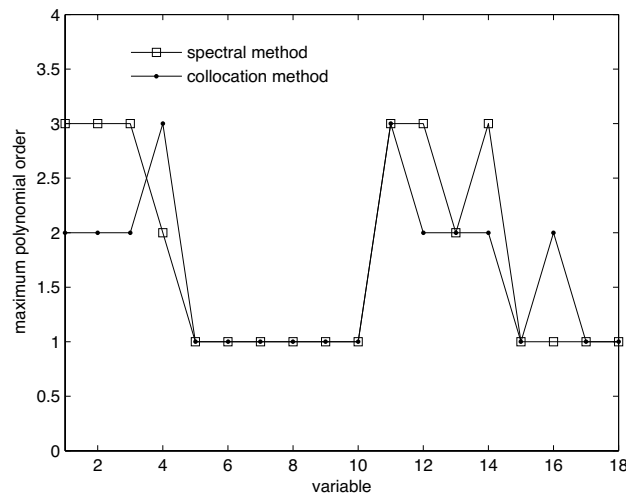


Figure 3. Maximum order polynomial reached in each variable for the stochastic spectral and collocation methods.

variable does not contribute to the variance as shown in Tables 3 and 5. Finally, the mean results are similar to the ones given by the spectral method (see Table 4).

7. CONCLUSION

The presence of uncertainties in the tissue properties has been analyzed in a 2D hyperthermia problem. Among the 18 uncertain properties, only those related to the tissues located in the neighborhood of the tumor have an impact on the repartition of the absorbed power. The sensitivity analysis made with fractional experimental designs leads to erroneous conclusions while the sensitivity and uncertainty analyses using the kriging technique give more accurate results. However, it appears that the spectral stochastic method is the best choice for this problem when it is used with an adaptive sparse grid algorithm: convergence is reached with about one hundred nodes. It has been shown that the implementation of the adaptative algorithm leads to an adaptative building of the polynomial chaos. On the contrary, using an adaptive sparse grid algorithm in a stochastic collocation method does not seem efficient but the reason is probably that the criterion for adaptivity used in this paper is not based on a statistical quantity; one should use a criterion based on the variance to improve the efficiency of the method. Finally, the 2D hyperthermia problem studied in this paper is useful to properly compare different methods and the conclusions here can be straightforwardly extended to other situations.

APPENDIX A. AN ADAPTIVE VERSION OF SMOLYAK'S ALGORITHM IN STOCHASTIC PROBLEMS

Consider a regular univariate function f . The integral of f on the interval $[-1, 1]$ can be approximated by a quadrature formula of level l :

$$\int_{-1}^1 f(x) dx \approx Q_l(f) = \sum_{k=1}^{n_l} w_{l,k} f(x_{l,k}) \quad (\text{A1})$$

where the $w_{l,k}$ and $x_{l,k}$ are respectively the weights and the abscissas related to quadrature nodes of level l ; accuracy increases with the level.

When the integration of regular functions in higher dimensions is considered, Smolyak's algorithm is usually preferred to the classical

tensor product of univariate quadrature formulas. Introducing the difference formulas:

$$\Delta_l(f) = Q_l(f) - Q_{l-1}(f) \text{ with } Q_0(f) = 0, \quad (\text{A2})$$

the conventional Smolyak algorithm to compute the integral of a d -variate function F on the hypercube $[-1, 1]^d$ is expressed by:

$$\int_{[-1, 1]^d} F(\mathbf{x}) d\mathbf{x} \approx \sum_{\mathbf{j} \in I(l)} \left(\otimes_{k=1}^d \Delta_{j_k} \right) (F) \quad (\text{A3})$$

with $\mathbf{j} = [j_1, \dots, j_d]$ and $I(l) = \{\mathbf{j} \mid |\mathbf{j}|_1 \leq l-1\}$ where $|\mathbf{j}|_1$ is the sum of the components j_k ; the k -th component j_k is such that $j_k + 1$ indicates the level of accuracy of the quadrature rule following the k -th variable; the symbol $\otimes_{k=1}^d \Delta_{j_k}$ denotes the tensor product of unidimensional quadrature rules.

In the adaptative version of the algorithm, the summation in (A3) is extended to more general admissible sets than $I(l)$. The only requirement for constructing these new admissible sets is that the difference formula $\Delta_{j_k} = Q_{j_k} - Q_{j_k-1}$ can be computed. Thus, a set of indices S is called admissible if, for all $\mathbf{j} \in S$, $\mathbf{j} - \mathbf{e}_k \in S$ for $1 \leq k \leq d$; \mathbf{e}_k is the k -th unit vector [15]. Following this definition, a general sparse grid formula becomes:

$$\int_{[-1, 1]^d} F(\mathbf{x}) d\mathbf{x} \approx \sum_{\mathbf{j} \in S} \left(\otimes_{k=1}^d \Delta_{j_k} \right) (F) \quad (\text{A4})$$

with S a given admissible set.

The idea of the adaptative algorithm is then to construct nested sequences of admissible sets. This construction is performed by adding in priority, to already computed indexes, the indexes in the forward neighborhood of the index with the largest estimated error; the forward neighborhood of an index \mathbf{j} is defined as the d indexes $\{\mathbf{j} + \mathbf{e}_k \mid k = 1, \dots, d\}$. This leads to the desired dimension-adaptive grid refinement. Newly added indexes are pooled as so-called *active indexes* while indexes of which the forward neighborhood has been processed become *old indexes*.

However, directly applying this algorithm in the case of the integrals of (4) needs some care. Each index \mathbf{j} coincides with a maximum degree of functions that can be exactly integrated; since the integrand is of the form $F = y\Psi_{\mathbf{i}}$ when evaluating $y_{\mathbf{i}}$, it implies that an index \mathbf{j} enables to compute $y_{\mathbf{i}}$ for a polynomial $\Psi_{\mathbf{i}}$ whose degree in each direction k is lower or equal to the value of the index \mathbf{j} in the

same direction: $i_k \leq j_k \forall k$. In other words, it means that as one moves forward in the algorithm, that is to say as the number of indexes \mathbf{j} for which the nodes have been computed increases, the number of terms $y_{\mathbf{i}}$ that are estimated increases in the same way. Using the notations given in [6], this specificity of the adaptative Smolyak algorithm is summarized in Algorithm 1. In this algorithm, O is the set of old indexes, A the set of active indexes, η the global error estimate, tol the error tolerance and l indicates a truncation limit of the polynomial chaos.

Algorithm 2 is another solution: it is more substantial but requires more calculation.

Algorithm 1 Adaptative algorithm. Version 1.

```

 $y_{\mathbf{i}}=0$  for  $\mathbf{i} \in I(l)$ 
 $\mathbf{j}=[0,\dots,0]$ 
for  $\mathbf{i} \in I(l)$  do
   $y_{\mathbf{i}} = y_{\mathbf{i}} + (\otimes_{k=1}^d \Delta_{j_k}) (y\Psi_{\mathbf{i}})$ 
5: end for
 $O = \emptyset$  ;  $A = \{\mathbf{j}\}$ 
 $\eta = +\infty$  ;  $g_{\mathbf{j}} = +\infty$  ;  $\sigma_y^2 = 0$ 
while ( $\eta \geq tol$ ) do
  select  $\mathbf{j}$  from  $A$  with largest  $g_{\mathbf{j}}$ 
10:  $A = A \setminus \{\mathbf{j}\}$ 
   $O = O \cup \{\mathbf{j}\}$ 
  for  $p=1,\dots,d$  do
     $\mathbf{h} = \mathbf{j} + \mathbf{e}_p$ 
    if  $\mathbf{h} - \mathbf{e}_q \in O$  for all  $q=1,\dots,d$  then
15:  $A = A \cup \{\mathbf{h}\}$ 
    for  $\mathbf{i} \in I(l)$  do
       $y_{\mathbf{i}} = y_{\mathbf{i}} + (\otimes_{k=1}^d \Delta_{h_k}) (y\Psi_{\mathbf{i}})$ 
    end for
     $\sigma_{y,\text{old}}^2 = \sigma_y^2$ 
20:  $\sigma_y^2 = \sum y_{\mathbf{i}}^2$  with  $\mathbf{i} \in O \cup A \setminus \{[0,\dots,0]\}$ 
     $g_{\mathbf{h}} = |\sigma_y^2 - \sigma_{y,\text{old}}^2|$ 
    end if
  end for
   $\eta = \max (g_{\mathbf{j}}/\sigma_y^2)$  with  $\mathbf{j} \in A$ 
25: end while

```

Algorithm 2 Adaptativealgorithm Version 2.

```

 $y_{\mathbf{i}} = 0$  for  $\mathbf{i} \in I(l)$ 
 $\mathbf{j} = [0, \dots, 0]$ 
for  $\mathbf{i} \in I(l)$  do
   $y_{\mathbf{i}} = y_{\mathbf{i}} + (\otimes_{k=1}^d \Delta_{j_k})(y\Psi_{\mathbf{i}})$ 
5: end for
 $O = \emptyset$ ;  $A = \{\mathbf{j}\}$ 
 $\varepsilon = +\infty$ ;  $g_{\mathbf{j}} = +\infty$ 
while ( $\eta \geq tol$ ) do
  select  $\mathbf{j}$  from  $A$  with largest  $g_{\mathbf{j}}$ 
10:  $A = A \setminus \{\mathbf{j}\}$ 
   $O = O \cup \{\mathbf{j}\}$ 
  for  $p = 1, \dots, d$  do
     $\mathbf{h} = \mathbf{j} + \mathbf{e}_p$ 
    if  $\mathbf{h} - \mathbf{e}_q \in O$  for all  $q = 1, \dots, d$  then
15:  $A = A \cup \{\mathbf{h}\}$ 
    for  $\mathbf{i} \in I(l)$  do
       $y_{\mathbf{i}} = y_{\mathbf{i}} + (\otimes_{k=1}^d \Delta_{h_k})(y\Psi_{\mathbf{i}})$ 
    end for
    end if
20: end for
 $AO^+ = A \cup O \setminus \{[0, \dots, 0]\}$ 
 $\sigma_y^2 = \sum y_{\mathbf{i}}^2$  with  $\mathbf{i} \in AO^+$ 
for  $\mathbf{j} \in A$  do
  for  $\mathbf{i} \in AO^+ \setminus \mathbf{j}$  do
25:  $y_{\mathbf{i}, \text{tamp}} = y_{\mathbf{i}} - (\otimes_{k=1}^d \Delta_{j_k})(y\Psi_{\mathbf{i}})$ 
  end for
   $\sigma_{y, \text{tamp}}^2 = \sum y_{\mathbf{i}}^2$  with  $\mathbf{i} \in AO^+ \setminus \mathbf{j}$ 
   $g_{\mathbf{j}} = |\sigma_y^2 - \sigma_{y, \text{tamp}}^2|$ 
end for
30:  $\eta = \max (g_{\mathbf{j}} / \sigma_y^2)$  with  $\mathbf{j} \in A$ 
end while

```

REFERENCES

1. Hurt, W. D., J. M. Ziriaux, and P. A. Mason, "Variability in EMF permittivity values: Implications for SAR calculations," *IEEE Trans. on Biomedical Engineering*, Vol. 47, No. 3, 396–401, 2000.
2. Garcia-Diaz, A. and D. Philips, *Principles of Experimental Design and Analysis*, Chapman & Hall, 1995.
3. Koehler, J. and A. Owen, *Handbook of Statistics*, 261–308,

- Chapter Computer experiments, Elsevier Science, 1996.
4. Ghanem, R. G. and P. D. Spanos, *Stochastic Finite Elements: A Spectral Approach*, Springer-Verlag, New York, 1991.
 5. Xiu, D. and J. S. Hesthaven, "High-order collocation methods for differential equations with random inputs," *SIAM Journal on Scientific Computing*, Vol. 27, No. 3, 1118–139, 2005.
 6. Gerstner, T. and M. Griebel, "Dimension-adaptive tensor-product quadrature," *Computing*, Vol. 71, No. 1, 65–87, Springer-Verlag, New York, Inc., 2003.
 7. IFAC, Institute For Applied Physics, <http://niremf.ifac.cnr.it/t-issprop/>.
 8. Stoneman, M. R., M. Kosempa, W. D. Gregory, C. W. Gregory, J. J. Marx, W. Mikkelson, J. Tjoe, and V. Raicu, "Correction of electrode polarization contributions to the dielectric properties of normal and cancerous breast tissues at audio/radiofrequencies," *Physical Medicine and Biology*, Vol. 52, 6589–6604, 2007.
 9. Renard, Y. and J. Pommier, "Getfem finite element library," <http://home.gna.org/getfem/>.
 10. OHagan, T. and M. Kennedy, "Gaussian emulator machine software," <http://www.tonyohagan.co.uk/academic/GEM/index.html>.
 11. Sobol, I. M., "Sensitivity estimates for non linear mathematical models," *Mathematical Modelling and Computational Experiments*, Vol. 1, 407–14, 1993.
 12. Xiu, D. and G. E. Karniadakis, "The Wiener-Askey polynomial chaos for stochastic differential equations," *SIAM Journal on Scientific Computing*, Vol. 24, No. 2, 619–44, (electronic), 2002.
 13. Zeng, Z. Y. and J. M. Jin, "An efficient calculation of scattering variation due to uncertain geometrical deviation," *Electromagnetics*, Vol. 27, No. 7, 387–398, 2007.
 14. Klimke, A., "Sparse grid interpolation toolbox," <http://www.ia-ns.uni-stuttgart.de/spinterp/>.
 15. Klimke, A., "Uncertainty modeling using fuzzy arithmetic and sparse grids," Ph.D. thesis, Fakultät Mathematik und Physik der Universität Stuttgart, 2006.